

C

Set	mRNA	CNV	R	FDR
LCI	2.5	28.1%	0.46	0.007
TCGA	2.4	26.8%	0.55	<0.0001

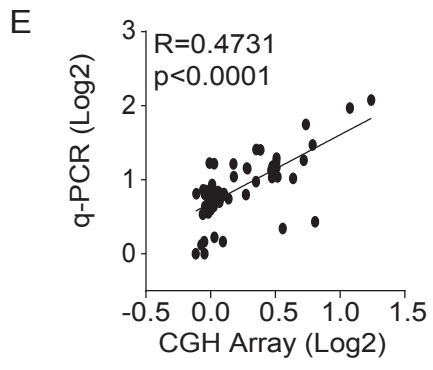
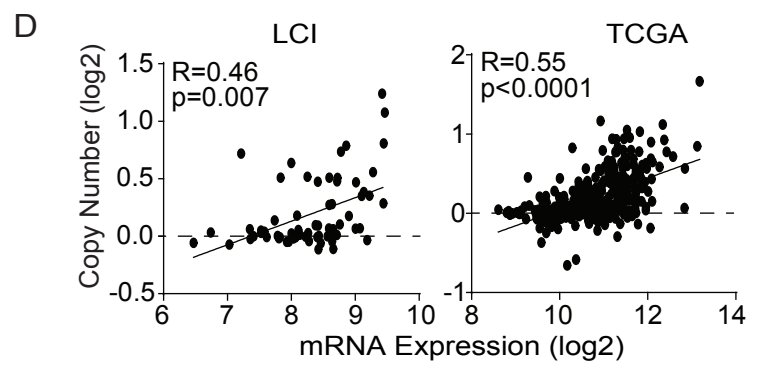
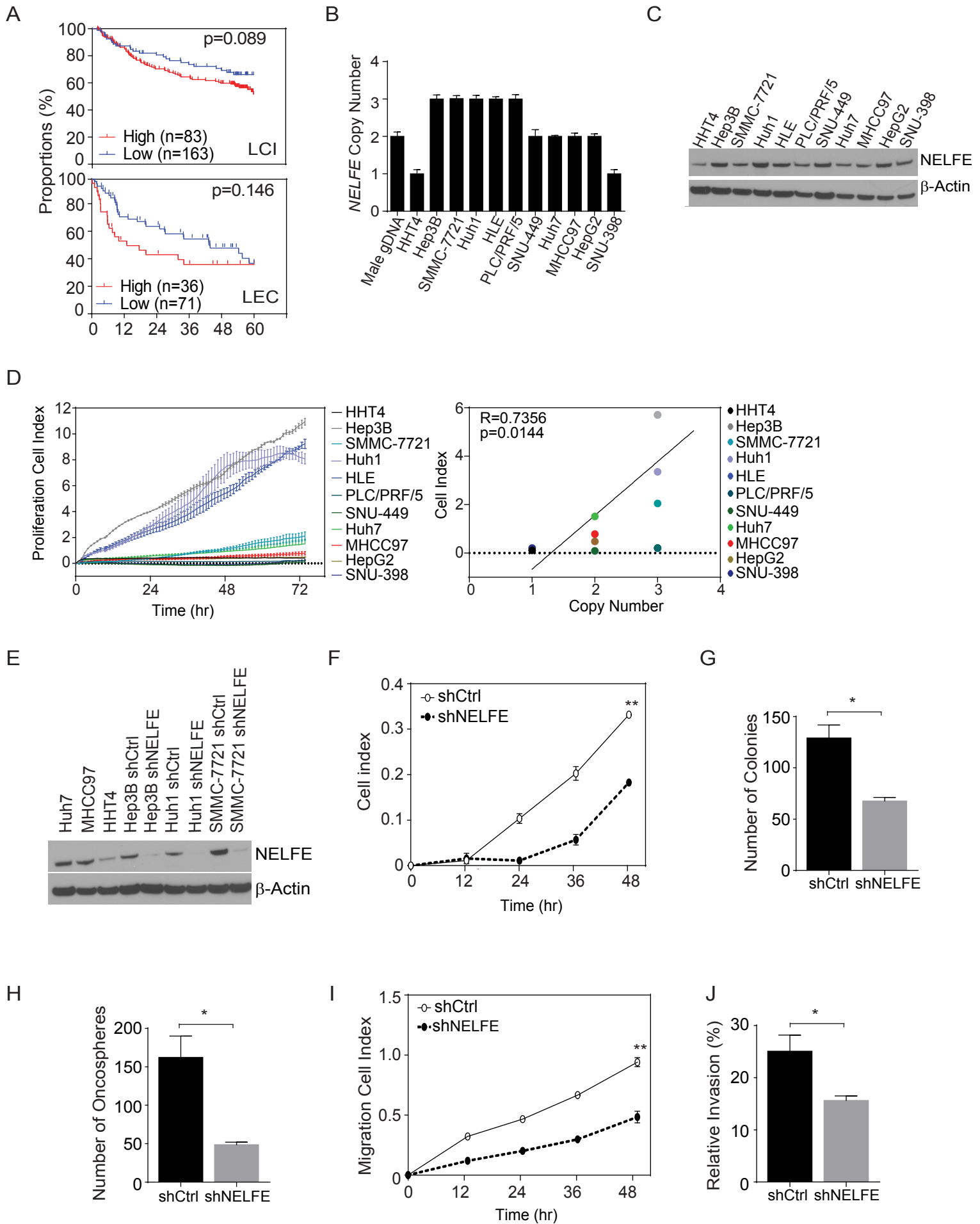
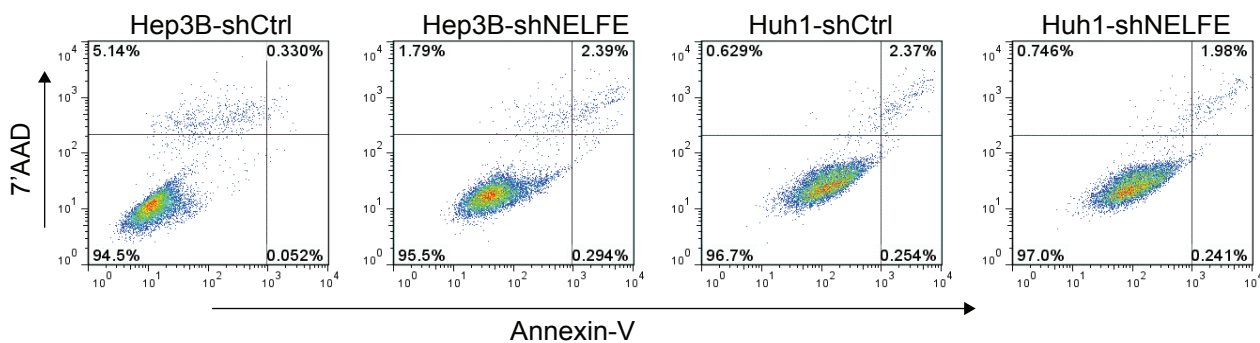


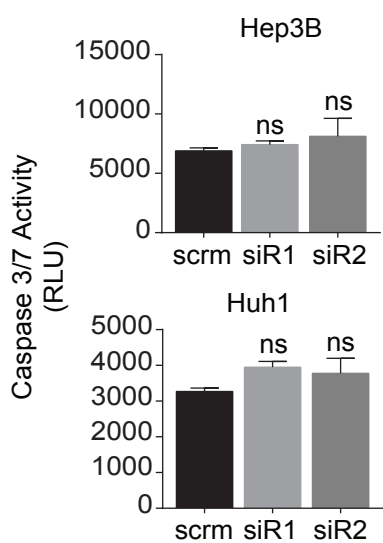
Figure S1, related to Figure 1. RBPs are ubiquitously altered in HCC. (A) Heatmap of the TCGA-LIHC and Stanford dataset from hierarchical clustering analysis of the 474 RBPs that are tumor specific. Pearson correlation with complete linkage was performed. (B) Kaplan-Meier curves of LCI cohort based on predictive survival analysis using the 629 transcription factors that were differentially expressed between tumor and non-tumor (p values are presented from Cox Log rank test). (C) Summary of NELFE expression, percentage of samples with amplification (calculated based on segment \log_2 values >0.32), Pearson correlation coefficient (R value) and FDR in two different datasets; LCI and TCGA. (D) Correlation of NELFE copy number from the LCI aCGH and microarray data from 64 HCC samples and TCGA-LIHC (SNP array compared to RNASeqV2, n=366). Pearson correlation (R) value and p values are depicted. (E) Correlation of NELFE copy number from aCGH and real-time polymerase chain reaction (RT-PCR) data from 64 HCC samples normalized to male gDNA. Pearson correlation (R) value and p values are depicted.



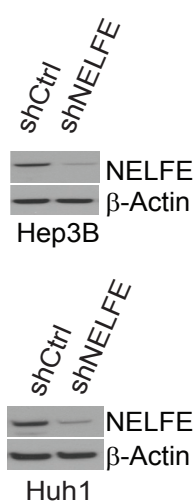
K



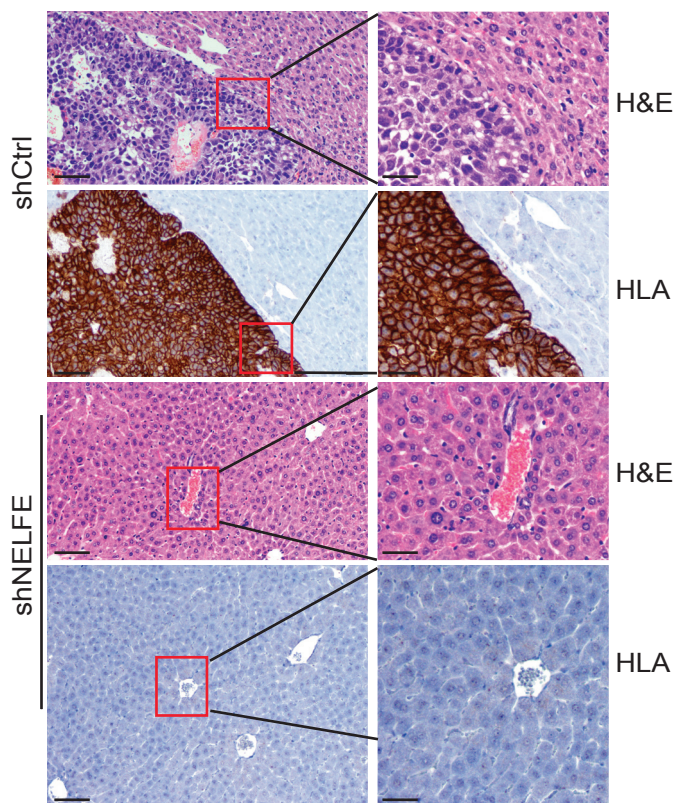
L



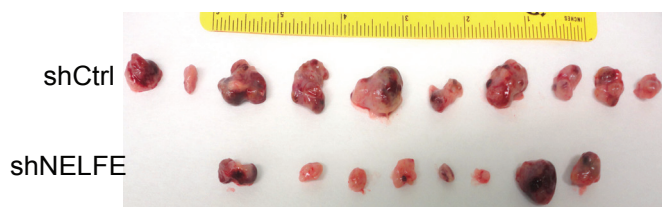
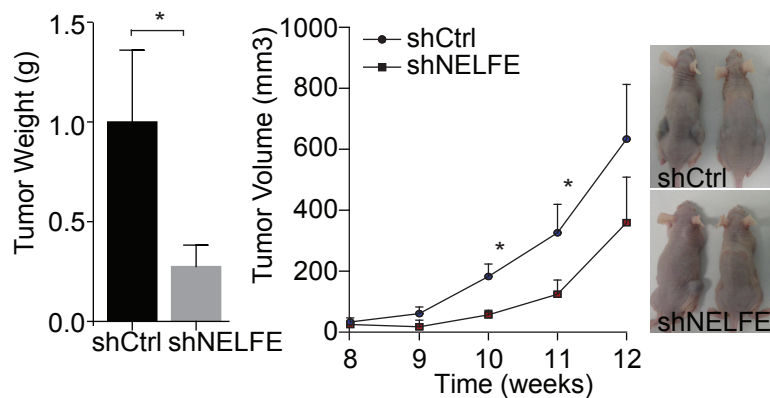
M



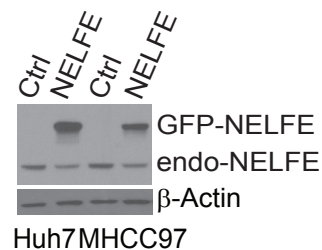
N



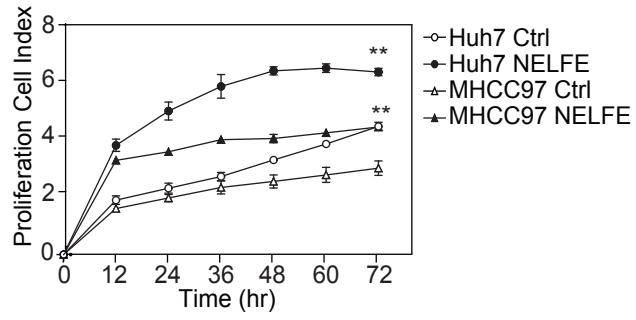
O



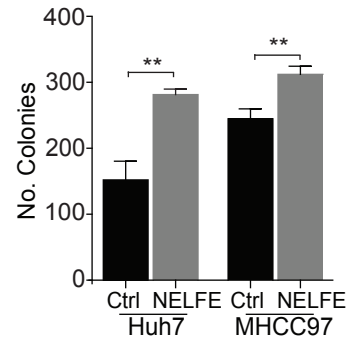
P



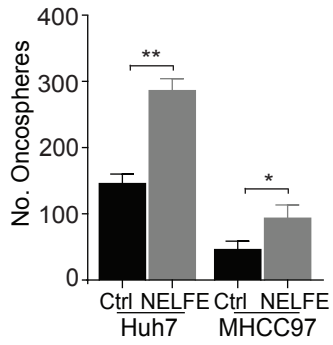
Q



R



S



T

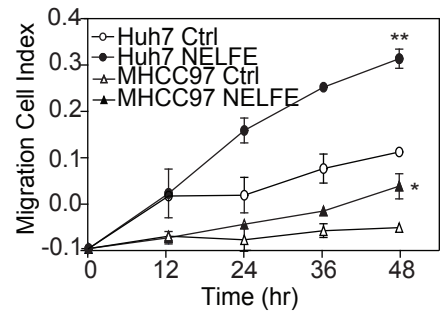
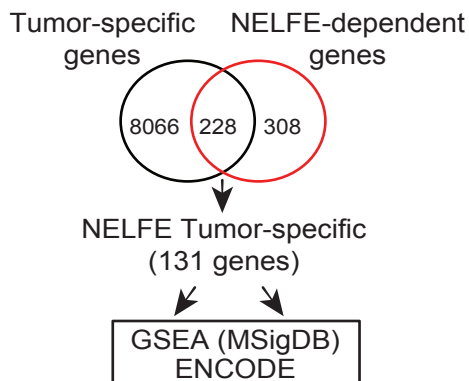
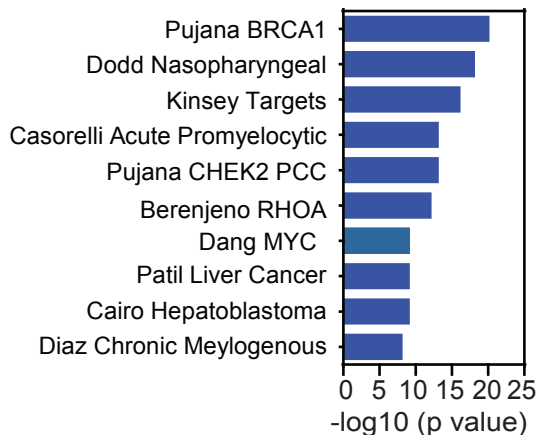


Figure S2, related to Figure 2. Alterations of NELFE in HCC cells. (A) Kaplan-Meier survival analysis of LCI and LEC cohort based on top 2/3 compared to bottom 1/3 values of NELFE (p values are presented from Cox Log rank test). (B) RT-PCR of male genomic DNA, eleven HCC cell lines, including the immortalized HHT4 normal hepatocyte cell line for NELFE gene copy number. (C) Immunoblot of NELFE and β -Actin of HCC cell lines and the hepatocyte HHT4 cell line. (D) Cell proliferation analysis of 11 cell lines via xCELLigence up to 72 hr. Correlation (Spearman rank test) plot of copy number as determined in compared to the cell index at 72 hr via xCELLigence. (E) Representative blot of HCC cells after 72 hr of NELFE shRNA and NELFE levels of HHT4, Huh7 and MHCC97 cells. (F) Cell proliferation analysis as measured by xCELLigence of SMMC-7721 cells with shCtrl or shNELFE knockdown after 48 hr (**p< 0.01). (G) Colony formation analysis after 10 days (**p< 0.01). (H) Oncosphere formation via Algimatrix after 10 days. 1×10^5 cells were plated for 10 days followed by crystal violet staining and manual counting (**p<0.01). (I-J) Cell migration and relative invasion analysis as measured by xCelligence after 48 hr (*p<0.01). (K) Flow cytometry analysis of Hep3B and Huh1 cells after 48 hr of NELFE siRNA compared to scrm control. Cells were stained with 7'AAD and Annexin-V. (L) Caspase 3/7 activity assay after 48 hr of siRNA mediated knockdown of NELFE compared to scrambled (scrm). (M) Immunoblot of pLKO.1 shNELFE or shCtrl Huh1 or Hep3B cells before injected into animals. (N) Representative microscopic images of mice livers after eight weeks of injection. H&E staining and immunohistochemistry of HLA-A, specific for human Huh1 HCC cells are shown. Scale bar, 100 μ M. (O) Hep3B cells were transfected with pLKO.1 shNELFE or shCtrl followed by 7 days of puromycin selection. Five million cells were subcutaneously injected bilaterally into the flanks of athymic nude mice. After 12 weeks, mice were sacrificed and all tumors formed are shown on the bottom panel. Tumor weight (right panel) after 12 weeks. Tumor volume (left panel) was measured using caliper weekly (*p<0.05) (shCtrl=10, shNELFE=8). (P) Immunoblot of NELFE in Huh7 and MHCC97 cells that have been stably transfected with lenti-mGFP-NELFE ORF (NELFE) or lenti-mGFP ORF (Ctrl). (Q) Cell proliferation as measured by xCELLigence after 72 hr (**p<0.01). (R) Colony formation of HCC cells (**p<0.01). (S) AlgiMatrixTM 3D Culture System was used for the oncospheroid formation assay for tumorigenic abilities of NELFE overexpression in HCC cells (*p<0.05, **p<0.01). (T) Cell migration assay determined by xCELLigence after 48 hr (*p<0.05, **p<0.01). All data are mean \pm SD.

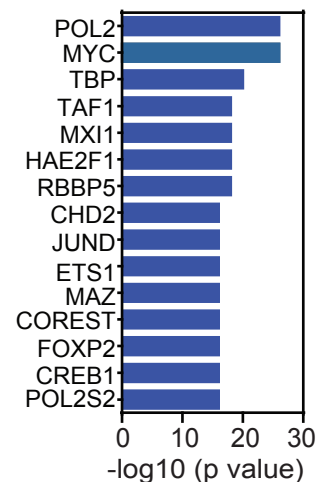
A



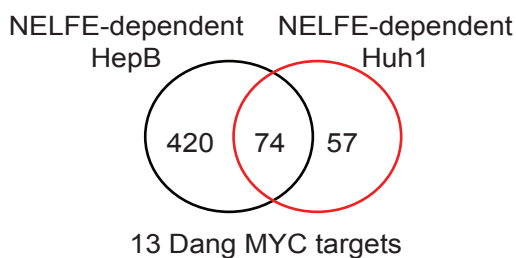
B



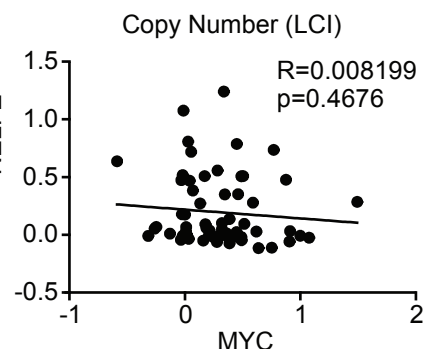
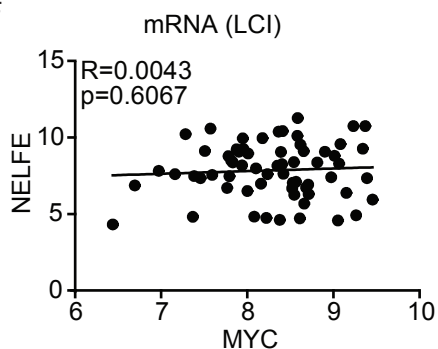
C



D

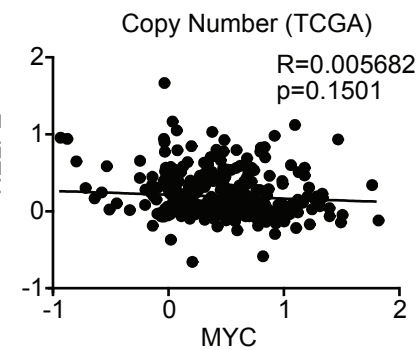
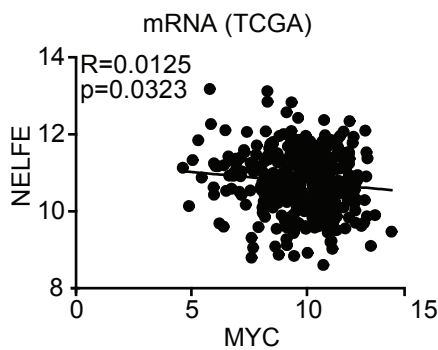


F

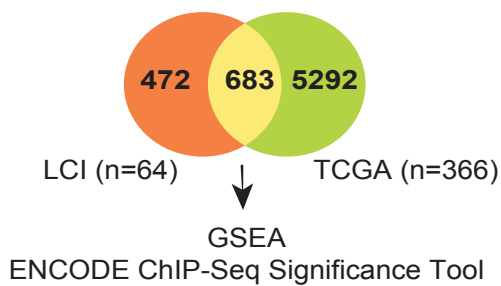


E

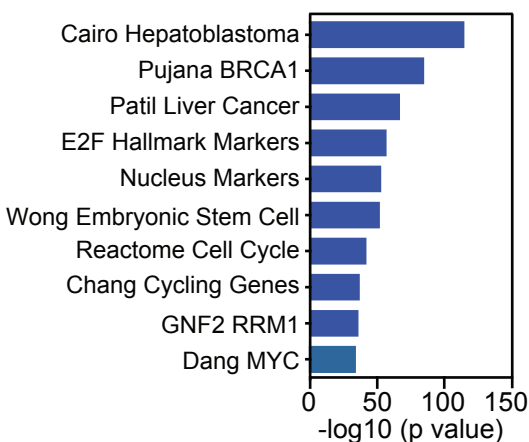
Gene	LCI	TCGA
Both	8/64(12.5%)	55/366(15%)
MYC	21/64(32.8%)	140/366(38%)
NELFE	11/64(17%)	39/366(10.8%)



G



H



I

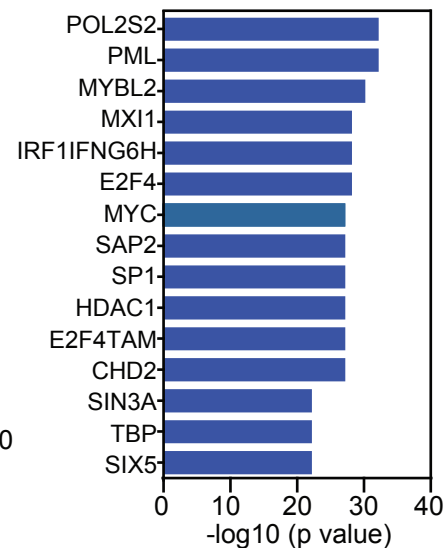


Figure S3, related to Figure 3. NELFE-dependent genes enhance MYC related genes. (A) Schematic of overview of microarray analysis using the Affymetrix HTA 2.0 genechip. The overlap of tumor specific genes from HCC clinical samples were compared to Huh1 NELFE siRNA treated cells. 131 genes were high in tumors but low after NELFE knockdown and vice versa were used for downstream analysis. (B) NELFE-dependent genes were enriched in MYC related genes and other HCC cancer specific signatures via GSEA analysis. (C) ENCODE analysis of 131 NELFE-dependent genes showing only the top 15 most enriched proteins including MYC. 90/131 genes are MYC related genes within 500 bp from the transcription start site. (D) 74 NELFE-dependent tumor-specific genes overlapped Hep3B and Huh1 cells, of which, 13 genes are also MYC target genes found in the Dang MYC target gene list. (E) Summary analysis of NELFE, MYC, or both NELFE/MYC gene copy alterations in HCC samples in the LIHC and TCGA-LIHC dataset. (F) Correlation analysis between NELFE and MYC mRNA levels and gene copy number alterations in the LCI and TCGA-LIHC dataset. R values are calculated using Pearson correlation analysis of log 2 values. (G) Schematic of overview of microarray analysis using the Affymetrix HTA 2.0 genechip looking at LCI cohort and TCGA-LIHC cohort. (H) GSEA analysis of 683 NELFE-dependent genes showing only the top 10 most enriched genesets. (I) ENCODE analysis of 683 NELFE-dependent genes showing only the top 15 most enriched proteins including MYC. Genes are MYC related genes within 500 bp from the transcription start site.

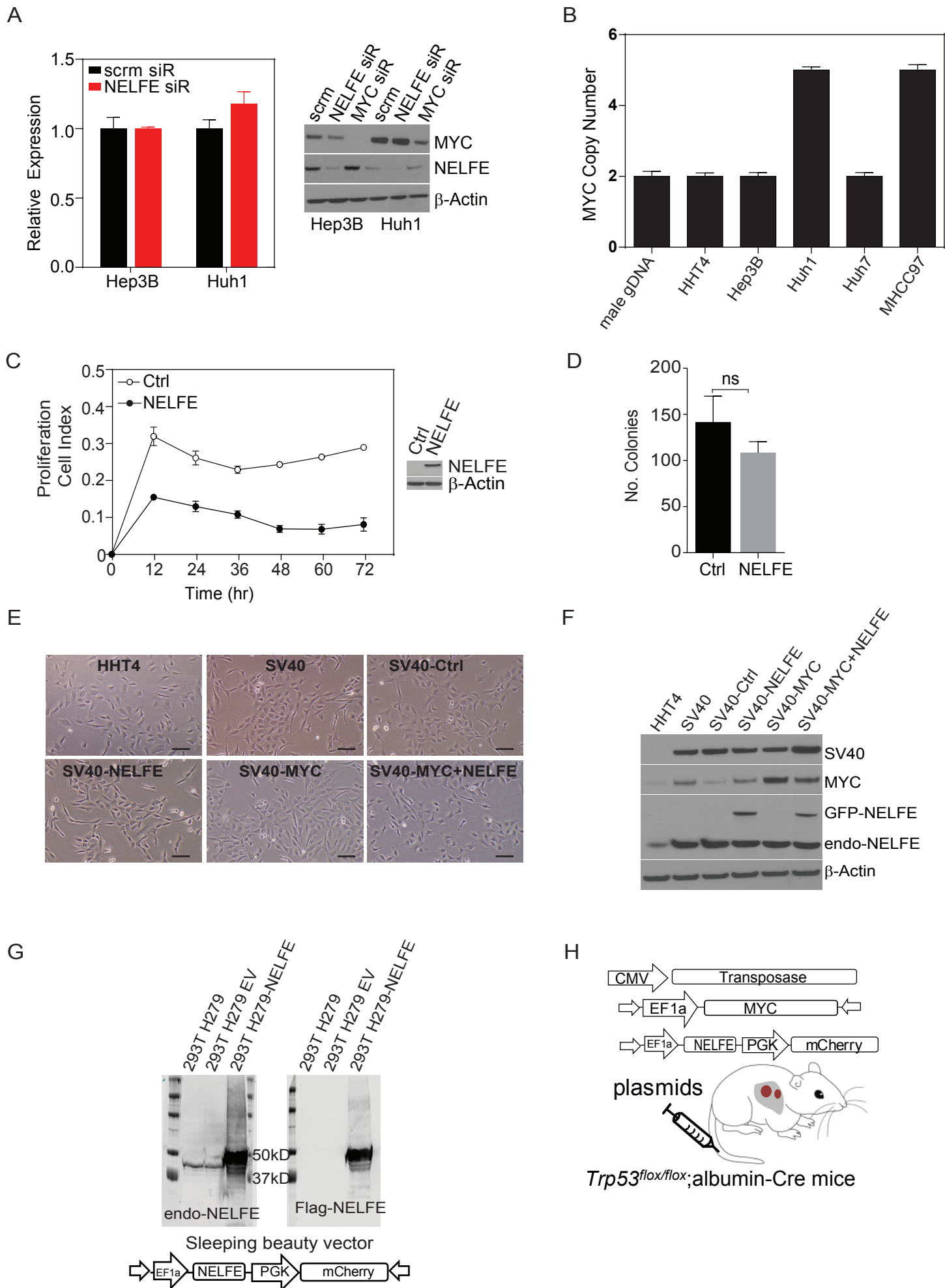
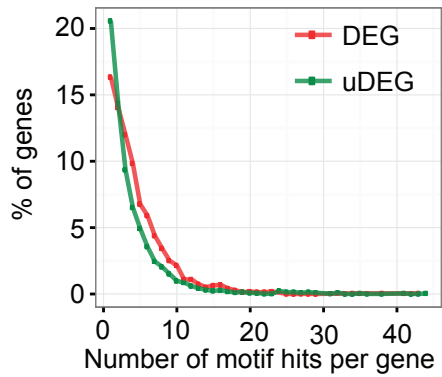


Figure S4, related to Figure 4. NELFE enhances MYC tumorigenic capabilities. (A) RT-PCR (left panel) and representative immunoblot (right panel) of MYC after 48 hr of NELFE siRNA compared to scrambled (scrm) control in HCC. (B) RT-PCR of MYC copy number in HCC cells compared to male gDNA. (C) Cell proliferation as measured by xCELLigence up to 72 hr (left panel) of HHT4 cells overexpressed with NELFE. Immunoblot of NELFE in HHT4 cells transfected with lenti-mGFP-NELFE ORF (NELFE) or lenti-mGFP ORF (Ctrl) (right panel). (D) Colony formation analysis after 10 days. (E) Phase contrast images of HHT4 transduced with SV40, SV40-Ctrl, SV40-NELFE, SV40-MYC, or SV40-MYC+NELFE. Scale bar, 200 μ M. (F) Immunoblot of NELFE in HHT4 cells transduced as specified. Representative Immunoblot of SV40, MYC, NELFE and β -Actin (endo-NELFE represents endogenous levels of NELFE). (G) Immunoblot of NELFE for confirmation of Sleeping beauty vectors with MYC or NELFE in HEK293T cells after transduction. (H) Cartoon of plasmid DNA which were tail-vein injected into 8 weeks old mice. All data are mean \pm SD.

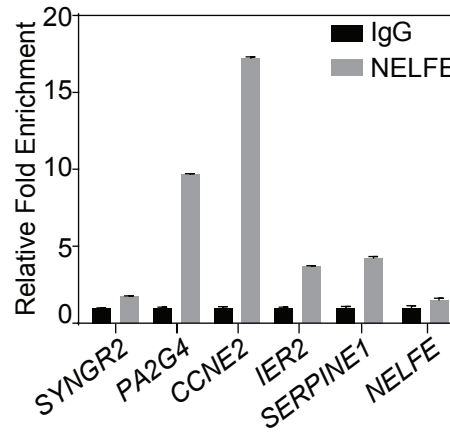
A



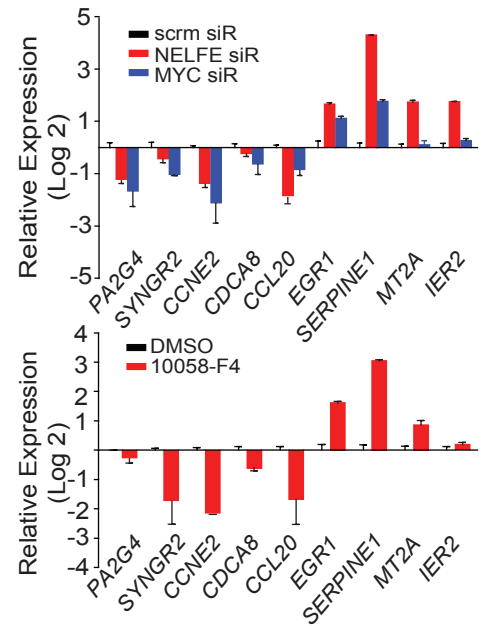
B



C



D



E

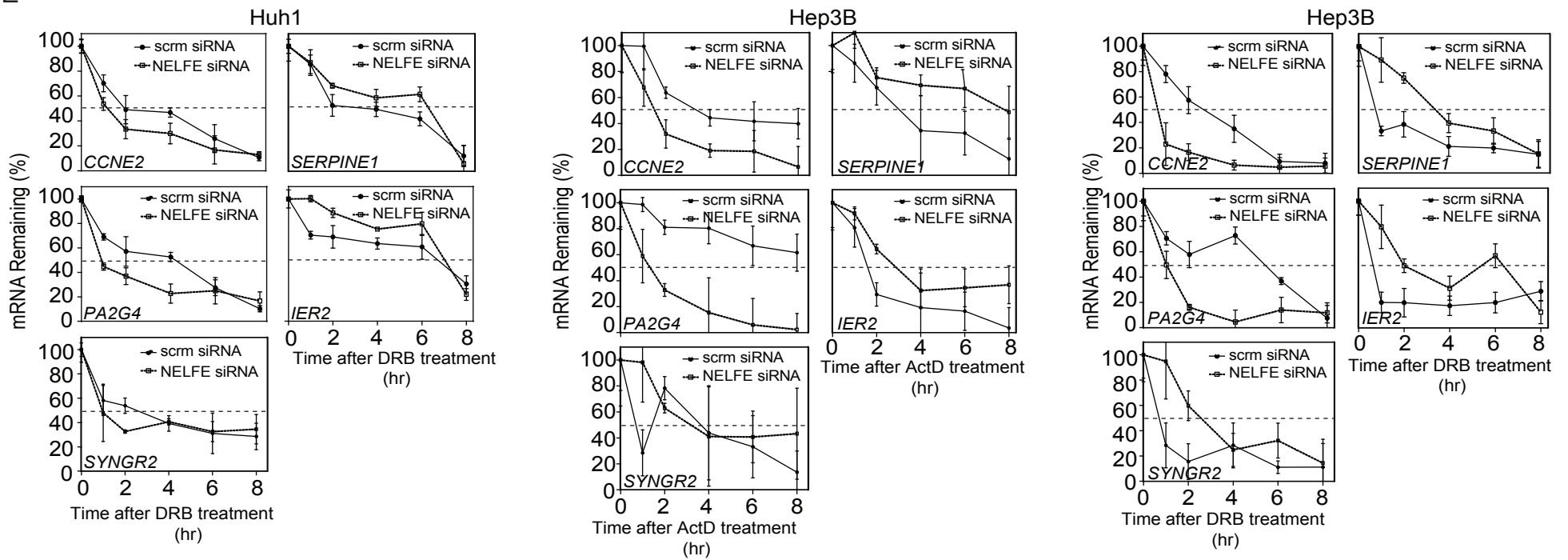
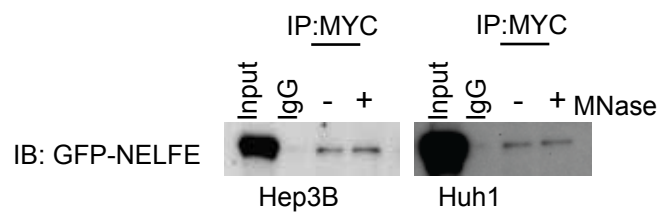


Figure S5, related to Figure 5. NELFE preferentially interacts with MYC related genes. (A) RNACompete analysis of differentially expressed genes (DEGs) and undifferentially expressed genes (uDEGs), which were determined previously by microarray analysis of Hep3B NELFE siRNA treatment vs. scrambled control. 2X2 table used to calculate Fishers exact test were performed to calculate p value. (B) The distribution of the number of motif hits per gene in DEGs or uDEGs. (C) Hep3B RNA immunoprecipitation followed by RT-PCR analysis of MYC related genes and NELFE predicted targets (*CCL20*, *PA2G4*, *CCNE2*, *IER2*, *SERPINE1*, *SYNGR2*). (D) Real-time PCR analysis (RT-PCR) of Huh1 cells after 72 hr of siRNA mediated knockdown of NELFE, MYC, or scramble control (scrm). Student's t-test was performed where treatments were compared to scrambled control (top panel). RT-PCR analysis of Huh1 cells after 16 hr of 10058-F4 (200 μ M) treatment compared to DMSO (bottom panel). Student's t-test was performed where treatments were compared to scrambled control (scrm). (E) RT-PCR of MYC related genes after NELFE siRNA compared to scrambled siRNA (scrm) followed by Actinomycin D treatment (10 μ g/ml) or DRB (50 μ M) treatment at different time points (0, 1, 2, 4, 6, 8 hr) in Huh1 and Hep3B cells. Dotted lines are at 50% mRNA remaining. All data are mean \pm SD.

A



B

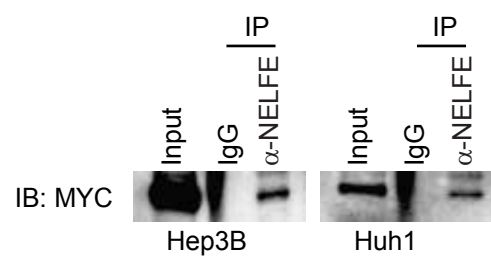


Figure S6, related to Figure 6. (A) Represented immunoblot of co-IP assay in Hep3B-mGFP-NELFE cells and Huh1-mGFP-NELFE cells with and without micrococcal nuclease treatment (MNase). MYC or Rabbit IgG was used for IP and mouse anti-NELFE was used for western blot. (B) Co-IP assay in Hep3B or Huh1 cells with NELFE or Mouse IgG to detect endogenous NELFE/MYC interaction. Rabbit anti-MYC was used for immunoblotting.